



# Graphene-based materials for energy applications

Jun Liu, Yuhua Xue, Mei Zhang, and Liming Dai

Accelerating global energy consumption makes the development of clean and renewable alternative energy sources indispensable. Nanotechnology opens up new frontiers in materials science and engineering to meet this energy challenge by creating new materials, particularly carbon nanomaterials, for efficient energy conversion and storage. Since the Nobel Prize winning research on graphene by Geim and Novoselov, considerable efforts have been made to exploit graphene as an energy material, and tremendous progress has been achieved in developing high-performance devices for energy conversion and energy storage. This article reviews recent progress in the research and development of graphene materials for advanced energy-conversion devices, including solar cells and fuel cells, and energy-storage devices, including supercapacitors and lithium-ion batteries, and discusses some challenges in this exciting field.

## Introduction

The development of clean and renewable energy is vital to meet ever-increasing global energy demands arising from rapid economic expansion and increasing world population, while minimizing fossil-fuel depletion, pollution, and global warming.<sup>1</sup> Currently, new technologies for energy conversion (e.g., solar cells and fuel cells) and energy storage (e.g., supercapacitors and batteries) are under intensive research. Because the performance of these devices depends strongly on the materials employed, various emerging nanomaterials with desired nanostructures and large surface/interface areas have been developed for applications in energy-related devices.<sup>2</sup> Of particular interest are carbon nanomaterials for energy applications.

Graphene, in particular, has received considerable attention because of its unique properties, including high thermal conductivity ( $\sim 5000 \text{ W m}^{-1} \text{ K}^{-1}$ ), high electrical conductivity ( $10^8 \text{ S m}^{-1}$ ), high transparency (absorbance of 2.3%), great mechanical strength (breaking strength of  $42 \text{ N m}^{-1}$  and Young's modulus of 1.0 TPa), inherent flexibility, high aspect ratio, and large specific surface area ( $2.63 \times 10^6 \text{ m}^2 \text{ kg}^{-1}$ ).<sup>3,4</sup> Graphene sheets of different sizes and defect contents can be prepared by various approaches, including manual mechanical cleavage of graphite with adhesive tape,<sup>3</sup> epitaxial growth on single-crystal SiC,<sup>5</sup> chemical vapor deposition (CVD) on metal surfaces,<sup>6</sup> oxidation–exfoliation–reduction of graphite powder,<sup>7</sup>

exfoliation of graphite through sonication/intercalation,<sup>8</sup> and organic coupling reactions.<sup>9</sup> Among these approaches, oxidation–exfoliation of graphite, followed by solution reduction, can be used to achieve large-scale production of graphene.<sup>8</sup> Graphene can also be readily doped with heteroatoms<sup>10</sup> (e.g., nitrogen, boron) or modified with organic molecules, polymers, or inorganic components.<sup>11</sup> The resultant soluble graphene derivatives can be processed into functional films by solution processing for many functional devices, such as sensors, actuators, field-effect transistors, solar cells, supercapacitors, and batteries.<sup>12–17</sup> In this article, we summarize progress in the development of graphene-based materials for energy-conversion and -storage applications and discuss some challenges in this exciting field.

## Graphene for energy conversion

It is estimated that the world will need to double its energy supply by 2050,<sup>1</sup> so it is of paramount importance to develop new types of energy sources. Compared to conventional energy materials, carbon nanomaterials exhibit unusual size- and surface-dependent (e.g., morphological, electrical, optical, and mechanical) properties that enhance energy-conversion performance. Specifically, considerable efforts have been expended to exploit the unique properties of graphene in high-performance energy-conversion devices, including solar cells and fuel cells.

Jun Liu, Department of Macromolecular Science and Engineering, Case Western Reserve University; jun.liu3@case.edu  
Yuhua Xue, Department of Macromolecular Science and Engineering, Case Western Reserve University; yxx110@case.edu  
Mei Zhang, Department of Biomedical Engineering, Case Western Reserve University; mxz128@case.edu  
Liming Dai, Department of Macromolecular Science and Engineering, Case Western Reserve University; liming.dai@case.edu  
DOI: 10.1557/mrs.2012.179

## Solar cells

Inorganic semiconductors, such as amorphous silicon, gallium arsenide, and sulfide salts, have been widely used in conventional photovoltaic cells, in which free electrons and holes are produced directly upon photon absorption.<sup>19</sup> Although a power conversion efficiency (PCE) of more than 40% has now been achieved for inorganic (III–V semiconductor) multijunction solar cells in the laboratory,<sup>20</sup> the widespread use of inorganic solar cells is still limited because of difficulties in modifying the bandgap of inorganic semiconductors and high costs associated with the elaborate fabrication processes involving elevated temperature and high vacuum.<sup>21</sup> These inorganic solar cells are still too expensive to compete with conventional grid electricity.<sup>22</sup> Alternative approaches using organic or polymer materials have received considerable attention because of their low cost, light weight, flexibility, and solution processability.<sup>23,24</sup>

### Polymer solar cells containing graphene

Unlike for their inorganic counterparts, photon absorption by conjugated polymers at room temperature often creates bound electron–hole pairs called excitons. Charge generation therefore requires dissociation of the excitons, a process that is known to be favorable at the interface between semiconducting materials with different ionization potentials and electron affinities (donors and acceptors).<sup>25</sup> Polymer solar cells (PSCs) often employ an active layer comprising a blend of donor and acceptor materials sandwiched between a cathode and an anode,<sup>26</sup> one of which must be transparent to allow sunlight to pass through. Upon illumination, photoinduced charge transfer between the donor and the acceptor leads to the generation of electrons and holes, which migrate to and are collected by the cathode and the anode, respectively. To facilitate charge collection by the electrodes, PSCs often require an electron-extraction layer between the cathode and the active layer, as well as a hole-extraction layer between the anode and the active layer.<sup>27</sup> **Figure 1a** shows the device structure of a typical PSC. Although PSCs still suffer from low PCEs, they have the great advantage of flexibility and low cost.

Carbon nanomaterials have been explored for several roles in solar cells. For example, indium tin oxide (ITO) is currently the most widely used transparent electrode in PSCs, but it suffers from brittleness and high production costs. The limited supply of indium in nature is another drawback for use of ITO electrodes. Large-area, continuous, single-layer or few-layer graphene sheets fabricated by CVD, with good transparency (>80%) and low sheet resistance (several hundred ohms per square), offer a potential inexpensive alternative for ITO as the transparent electrode.<sup>28–30</sup> In this context, layer-by-layer stacked

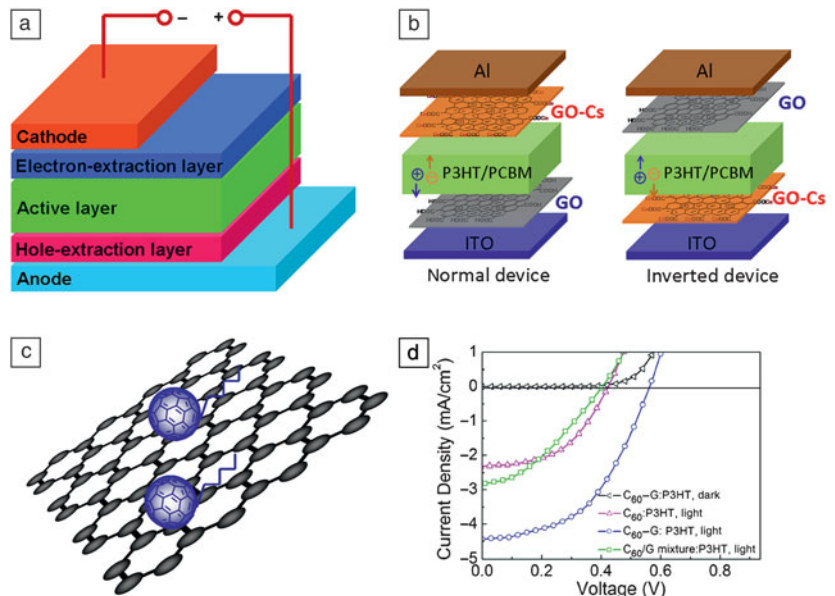


**Figure 1.** (a) Device structure of a polymer solar cell (PSC) in the normal configuration. (b) Device structures of (left) normal and (right) inverted PSCs with graphene oxide (GO) as the hole-extraction layer and cesium-neutralized graphene oxide (GO-Cs) as the electron-extraction layer. ITO, indium tin oxide; P3HT, poly(3-hexylthiophene); PCBM, [6,6]-phenyl-C<sub>61</sub>-butyric acid methyl ester. Parts (a) and (b) reproduced with permission from Reference 32. ©2012, Wiley. (c) Illustration of C<sub>60</sub>-grafted graphene (C<sub>60</sub>-G) and (d) its PSC device performance under AM1.5G illumination (the standard spectrum at Earth's surface, including both direct and diffuse radiation). Parts (c) and (d) reproduced with permission from Reference 35. ©2011, American Chemical Society.

graphene grown on a copper foil and doped with acid to provide carriers was reported to exhibit a sheet resistance of 80 Ω/sq and a transmittance of 90% at 550 nm.<sup>28</sup> PSCs employing this layered graphene electrode and MoO<sub>3</sub> as a hole-extraction layer showed a PCE of 2.5%.

Graphene oxide (GO) derivatives have also been demonstrated to be excellent hole- and electron-extraction layers in PSCs.<sup>31–33</sup> As a hole-extraction layer, GO has been used to achieve a PCE comparable to that of the state-of-the-art poly(3,4-ethylenedioxythiophene):poly(styrene sulfonate) (PEDOT:PSS) layer.<sup>31</sup> On the other hand, cesium-neutralized graphene oxide (GO-Cs), obtained through simple charge neutralization of the peripheral carboxylic acid groups of GO with Cs<sub>2</sub>CO<sub>3</sub>,<sup>32</sup> was demonstrated to act as an excellent electron-extraction layer. PSCs with GO and GO-Cs as the hole- and electron-extraction layers, respectively, exhibited a PCE of 3.67%, a value that is comparable to that (3.15%) of corresponding devices with state-of-the-art hole- and electron-extraction layers.<sup>32</sup>

Graphene derivatives have also been used in the active layers of PSCs.<sup>34–37</sup> For example, Yu et al.<sup>34</sup> chemically grafted CH<sub>2</sub>OH-terminated regioregular poly(3-hexylthiophene) (P3HT) onto carboxyl groups of GO through an esterification reaction to produce P3HT-grafted graphene sheets (G-P3HT). A solution-cast bilayer photovoltaic device based on C<sub>60</sub>-G:P3HT exhibited twice the PCE (0.61%) of its

$C_{60}$ :P3HT counterpart under AM1.5G illumination (the standard spectrum at Earth's surface, including both direct and diffuse radiation). The same authors also developed  $C_{60}$ -grafted graphene nanosheets ( $C_{60}$ -G) through a simple lithiation reaction (Figure 1c). The resultant  $C_{60}$ -G material was used as the electron acceptor in a P3HT-based bulk heterojunction solar cell to significantly improve the electron transport and, hence, the overall device performance (Figure 1d).<sup>35</sup> Efficient photoinduced charge transfer from the P3HT polymer donor to the graphene acceptor was also reported for PSCs with phenyl isocyanate functionalized graphene oxide as the acceptor.<sup>36</sup> The device performance was found to depend strongly on several factors, including the concentration of graphene, annealing time, and annealing temperature. On the other hand, an electrochemistry approach was recently used to develop graphene quantum dots, which can also be used as an acceptor in PSCs.<sup>37</sup>

### Graphene–inorganic quantum dot hybrid solar cells

Inorganic quantum dot (QD) solar cells represent a promising photovoltaic technology because of their potential to exceed the Shockley–Queisser limit on single-junction energy extraction from the solar spectrum, their size-tunable photon absorption, and their efficient generation of multiple electron–hole pairs.<sup>38</sup> However, QD solar cells currently suffer from low photovoltaic efficiency because of poor electron–hole separation and deficient transfer of photogenerated electrons to electrodes. Although single-walled carbon nanotubes (SWNTs), stacked SWNTs with suitable energy levels, and one-dimensional nanostructures have been used as electron acceptors in QD solar cells to improve electron–hole separation, these devices still exhibited low incident photon-to-charge-carrier conversion efficiencies (IPCEs) of <5% and a photocurrent response of 4 A/m<sup>2</sup> under 1000 W/m<sup>2</sup> illumination.<sup>38</sup> Using graphene as a novel electron acceptor, Guo et al.<sup>39</sup> developed QD solar cells with the multilayered graphene–QD device structure and energy level alignment shown in Figure 2a and 2c, respectively. Owing

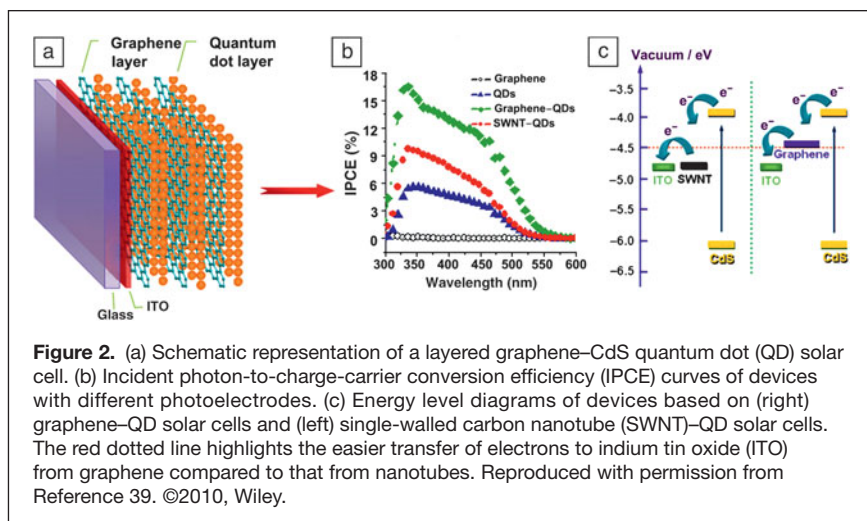
to the high specific surface area, high mobility, and tunable bandgap of graphene, the resulting device exhibited an IPCE as high as 16% and a photoresponse of 10.8 A/m<sup>2</sup> under 1000 W/m<sup>2</sup> illumination (Figure 2b). This achievement represents significant progress in the development of high-performance QD solar cells. Further research efforts in this area could lead to even higher efficiencies.

### Dye-sensitized solar cells containing graphene

Dye-sensitized solar cells (DSSCs) represent a relatively new class of low-cost solar cells with great promise. As shown in Figure 3, a typical DSSC consists of a transparent cathode (e.g., fluorine-doped tin oxide [FTO]), a highly porous semiconductor (e.g., TiO<sub>2</sub>) layer with a soaked layer of dye (e.g., ruthenium polypyridine dye), an electrolyte solution containing redox pairs (e.g., iodide/triiodide), and a counter electrode (e.g., platinum). In operation, a dye molecule harvests sunlight and is excited to inject an electron directly into the conduction band of the TiO<sub>2</sub>. The injected electron then moves to the transparent anode and, through the external circuit, to the cathode (Figure 3). Meanwhile, the dye molecule strips one electron from iodine in the electrolyte by oxidizing it to triiodide. The triiodide then recovers its missing electron from the external circuit by diffusing to the counter electrode (i.e., cathode).<sup>40</sup> The recently reported highest PCE for a DSSC is 12.3%.<sup>41</sup> Although DSSCs are still not as efficient as silicon solar cells, their low cost and easy fabrication have made them very attractive for “low-density” applications, including rooftop solar collectors. As discussed in the remainder of this section, graphene has been used in almost every component of a DSSC.

In view of the aforementioned high transparency and good conductivity intrinsically associated with graphene, several groups have applied graphene as a transparent cathode in DSSCs. For instance, Wang et al.<sup>42</sup> processed solutions of reduced graphene oxide to deposit graphene films with a moderate conductivity of about  $5.5 \times 10^4$  S/m and a high transmittance of 80%. They used these films as transparent electrodes in DSSCs that exhibited a lower PCE than achieved by an FTO-based device (0.26% for graphene film versus 0.84% for FTO).

The counter electrode of a DSSC catalyzes the reduction of redox pairs after electron injection. The state-of-the-art counter electrode, platinum, is very expensive. As alternatives, graphene-modified FTO and a graphene–conjugated polymer composite film have been used as counter electrodes to create DSSCs with iodine/triiodide redox pairs, providing performances better than unmodified FTO or bare polymer but still worse than that of platinum-coated FTO.<sup>43,44</sup> Recently, DSSCs with Co<sup>2+/3+</sup> redox pairs were reported to exhibit a higher open-circuit voltage and a higher PCE than the iodine/triiodide counterpart with the same type



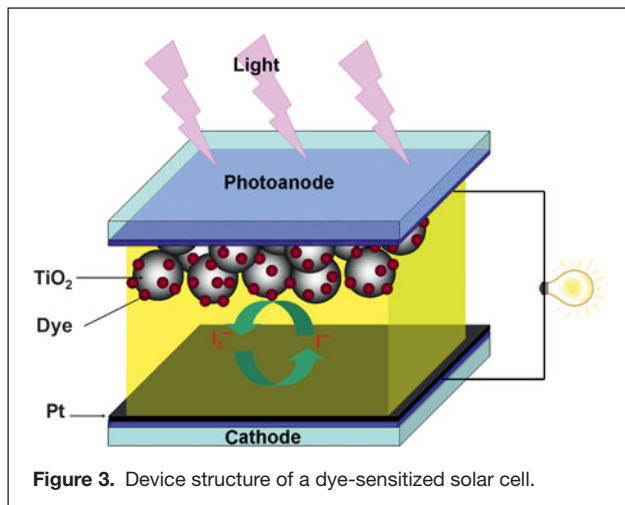


Figure 3. Device structure of a dye-sensitized solar cell.

of counter electrode. Kavan et al.<sup>45</sup> found that, for  $\text{Co}^{2+/3+}$  redox pairs, a graphene film on FTO exhibited higher electrocatalytic activity and higher device efficiency than a platinum–FTO electrode at high illumination intensity, indicating that graphene is an excellent counter electrode material for DSSCs.

The good conductivity of graphene can also be used to facilitate electron transport in porous  $\text{TiO}_2$  layers.<sup>46,47</sup> For example, incorporation of graphene into  $\text{TiO}_2$  layers was found to lead to a 45% increase in short-circuit current and a 39% increase in PCE due to lower recombination, faster electron transport, and higher light scattering.<sup>46</sup> In addition, graphene quantum dots have been used as light absorbers in DSSCs.<sup>48</sup>

### Fuel cells

Fuel cells are considered to be one of the most efficient and environmentally benign energy-conversion technologies. Instead of burning fuel to create heat, fuel cells convert chemical energy directly into electricity, and with no moving parts, fuel cells produce no air pollution, hazardous wastes, or noise. As shown in **Figure 4a**, when hydrogen gas, for example, is pumped onto one electrode (the anode), the hydrogen is split into its constituent electrons and protons. The protons diffuse through the cell toward a second electrode (the cathode), whereas the electrons flow out of the anode to provide electrical power. Electrons and protons both end up at the cathode, where they combine with oxygen to form water.

The oxygen reduction reaction (ORR) can proceed either through a four-electron process that directly combines oxygen with electrons and protons to form water or through a less efficient two-step, two-electron pathway involving the formation of hydrogen peroxide ions as an intermediate.<sup>42</sup> The ORR would naturally occur very slowly without a catalyst on the cathode. Platinum nanoparticles have long been regarded as the best catalyst for the ORR, although platinum-based electrodes suffer from a susceptibility to time-dependent drift and CO deactivation.<sup>49</sup> The high cost of platinum catalysts is also an obstacle to mass-market fuel cells for commercial applications.

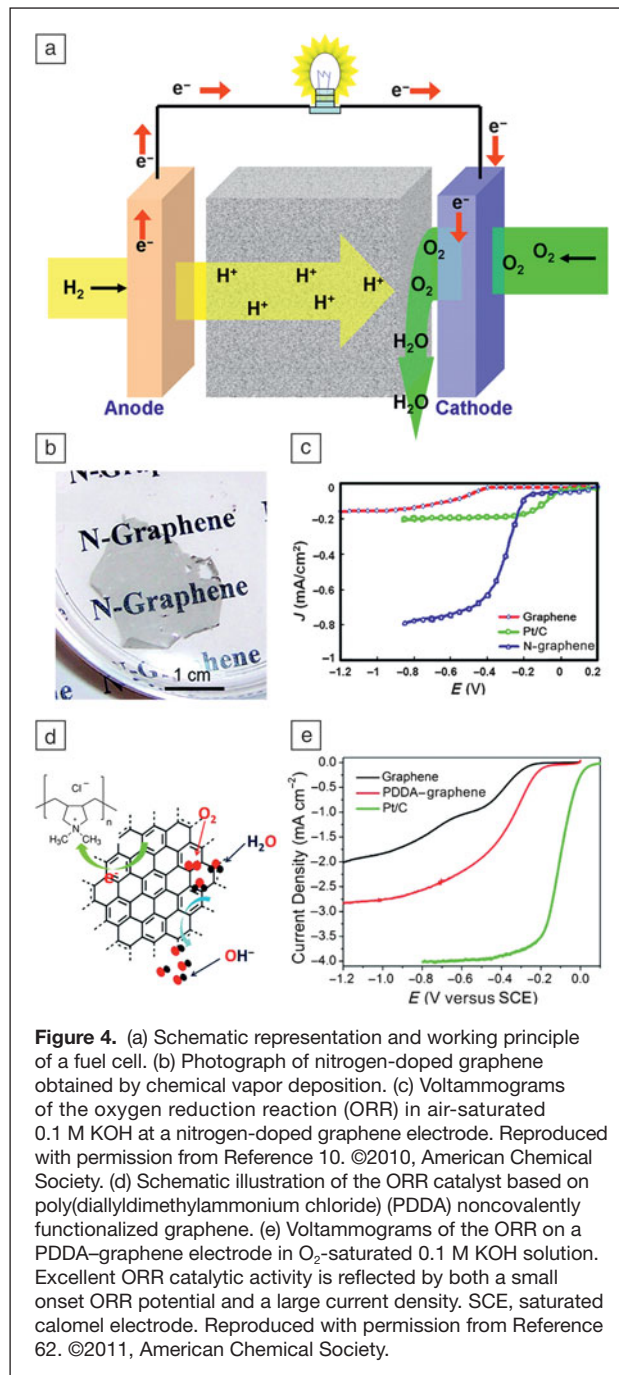


**Figure 4.** (a) Schematic representation and working principle of a fuel cell. (b) Photograph of nitrogen-doped graphene obtained by chemical vapor deposition. (c) Voltammograms of the oxygen reduction reaction (ORR) in air-saturated 0.1 M KOH at a nitrogen-doped graphene electrode. Reproduced with permission from Reference 10. ©2010, American Chemical Society. (d) Schematic illustration of the ORR catalyst based on poly(diallyldimethylammonium chloride) (PDPA) noncovalently functionalized graphene. (e) Voltammograms of the ORR on a PDDA-graphene electrode in  $\text{O}_2$ -saturated 0.1 M KOH solution. Excellent ORR catalytic activity is reflected by both a small onset ORR potential and a large current density. SCE, saturated calomel electrode. Reproduced with permission from Reference 62. ©2011, American Chemical Society.

Indeed, the large-scale practical application of fuel cells has not been realized, even though alkaline fuel cells with platinum as an ORR electrocatalyst were developed for the Apollo lunar missions in the 1960s. Recent intensive research efforts to reduce or replace platinum-based electrodes in fuel cells have led to the development of new metal-free ORR electrocatalysts based on carbon nanomaterials. In particular, nitrogen-doped graphene was found to be a promising alternative metal-free ORR catalyst with a better electrocatalytic activity, longer operation stability, and greater tolerance to crossover of fuel from the opposite electrode than platinum.<sup>10</sup>

### Fuel cells with graphene as the catalyst support

To improve the activity and efficiency of platinum catalysts, a widely used approach has been to immobilize platinum components on a highly conducting substrate that is inexpensive and has a high specific surface area.<sup>50–52</sup> In this context, platinum nanoparticles supported on graphene sheets were found to exhibit a higher electrochemical surface area and ORR activity and better stability than the commercial platinum catalyst from the E-TEK division of BASF Fuel Cell.<sup>50</sup> The observed excellent ORR performance was attributed to the smaller size and reduced aggregation of platinum nanoparticles immobilized on the graphene sheets. Jafri et al.<sup>51</sup> used graphene nanoplatelets and nitrogen-doped graphene nanoplatelets as supports for platinum nanoparticles to construct proton-exchange membrane fuel cells with power densities of 4400 W/cm<sup>2</sup> and 3900 W/cm<sup>2</sup>, respectively. The better performance of the nitrogen-doped graphene nanoplatelets was attributed to pyrrolic nitrogen defects (in which the nitrogen contributes two lone-pair electrons to the  $\pi$  system) acting as anchoring sites for carbon-catalyst binding and increasing electrical conductivity. To address the problem of CO deactivation of platinum catalysts, Dong et al.<sup>52</sup> developed graphene-supported platinum–ruthenium nanoparticles that also provide higher electrocatalytic performance with reduced overpotential and improved reversibility compared to graphite-supported alternatives.

### Fuel cells with nitrogen-doped graphene as the metal-free catalyst

Apart from their use as catalyst supports, graphene and related materials have recently attracted significant attention as metal-free catalysts for fuel cells. For example, Gong et al.<sup>53</sup> found that vertically aligned nitrogen-doped carbon nanotubes (VA-NCNTs) can effectively catalyze a four-electron ORR process with a much higher catalytic activity, lower overpotential, smaller crossover sensitivity, and better long-term operation stability than commercially available platinum/carbon black catalysts (brand name C2-20, 20% platinum on Vulcan XC-72R, E-TEK).<sup>53</sup> The success of VA-NCNTs as ORR catalyst has motivated investigations of nitrogen-doped graphene for the same application.

According to quantum-mechanics calculations, carbon atoms adjacent to nitrogen dopants in VA-NCNTs have a relatively high positive charge density to counterbalance the strong electron affinity of the nitrogen atom. Nitrogen-induced charge delocalization can change the electrochemical potential and the chemisorption mode of O<sub>2</sub> to weaken the oxygen–oxygen bonding, hence facilitating the ORR. Therefore, doping CNTs with nitrogen heteroatoms efficiently creates metal-free active sites for the electrochemical reduction of O<sub>2</sub>.<sup>53</sup>

Uncovering this new ORR mechanism for VA-NCNTs is important, as the same principle can be applied to other carbon nanomaterials (e.g., graphene). Indeed, nitrogen-doped graphene films produced by CVD in the presence of ammonia provide superb ORR performance, similar to that of VA-NCNTs at the same nitrogen content in alkaline medium (Figure 4b–c).<sup>10</sup> Nitrogen-doped graphene samples synthesized

by other approaches, including nitrogen plasma treatment of graphene,<sup>54</sup> edge functionalization of graphene,<sup>55</sup> thermal treatment of graphene with ammonia,<sup>56</sup> and solvothermal treatment of graphene with tetrachloromethane and lithium nitride,<sup>57</sup> also show good ORR electrocatalytic activities.

Recent work indicates that graphene and its derivatives doped with heteroatoms other than nitrogen could also exhibit improved ORR electrocatalytic activities, as exemplified by phosphorous-doped graphite layers,<sup>58</sup> boron-doped carbon nanotubes,<sup>59</sup> and sulfur-doped graphene.<sup>60</sup> More recently, Wang and co-workers<sup>61</sup> successfully produced graphene codoped with nitrogen and boron (BCN graphene) by simply annealing graphene oxide in the presence of boric acid under ammonia and demonstrated significantly improved ORR electrocatalytic activity, even better than that of a commercial platinum/carbon electrode, resulting from a poorly understood synergistic effect associated with nitrogen and boron codoping of graphene.

Apart from such heteroatom-induced intramolecular charge transfer, charge transfer between molecules has also been demonstrated to impart ORR electrocatalytic activity to graphene. In particular, graphene functionalized with poly(diallyldimethylammonium chloride) (PDDA) was reported to exhibit good ORR electrocatalytic activity (Figure 4d–e) resulting from charge transfer between the N-free graphene and PDDA. Such intermolecular charge transfer provides a simple, low-cost approach to develop carbon-based metal-free ORR catalysts. Continued research in this nascent field could give rise to a flourishing advanced energy-conversion technology based on graphene materials.

### Graphene for energy storage

Along with energy conversion, energy storage (as in supercapacitors and batteries) is also of paramount importance, especially for mobile applications. For many practical applications, high energy-storage capability, high power-delivery capability, and long cycle life are necessary. Owing to the unique characteristics of graphene, much effort has been devoted to applications of graphene in high-performance supercapacitors and batteries.

#### Supercapacitors

Supercapacitors are electrochemical devices that can store energy and release it with high power capability and high current density within a short time interval.<sup>63</sup> Thus, supercapacitors are considered to be the perfect complement for batteries or fuel cells in various applications, such as automobiles and high-performance portable electronics. The principle of energy storage in a supercapacitor is either (1) electrostatic charge accumulation on the electrode–electrolyte interface (electric double-layer capacitance) or (2) transfer of charge to the layer of redox molecules on the surface of the electrode (pseudocapacitance). In practical supercapacitors, the two storage mechanisms often work simultaneously.<sup>64</sup> Electrode materials intensively studied for supercapacitors include carbon,<sup>65</sup> metal oxides,<sup>66</sup> and conducting polymers,<sup>67</sup> with a recent focus on CNTs and graphene.

### Supercapacitors with graphene electrodes

The electric double-layer capacitance is proportional to the effective specific surface area of an electrode material. Therefore, graphene, with a theoretical specific surface area of  $2.63 \times 10^6 \text{ m}^2/\text{kg}$ , together with good conductivity, controllable microstructure, and excellent thermal/mechanical stability, is promising for supercapacitor electrodes.<sup>68–71</sup> Using a chemically reduced graphene oxide electrode, Stoller et al.<sup>68,69</sup> obtained specific capacitances of 135,000 F/kg and 99,000 F/kg in aqueous and organic electrolytes, respectively. They also obtained capacitance values of 191,000 F/kg and 120,000 F/kg in organic electrolytes for reduced graphene oxides produced using simple microwave heating and propylene carbonate solution reduction, respectively. On the other hand, Wang et al.<sup>71</sup> reported graphene-based supercapacitors with a maximum specific capacitance of 205,000 F/kg at a power density of 10 kW/kg and an energy density of 28.5 W h/kg that also had an excellent cyclic lifetime, retaining 90% of the initial capacitance after 1200 cycles.

### Supercapacitors with carbon nanotube and graphene hybrid electrodes

Hybrid electrodes based on two-dimensional graphene and one-dimensional carbon nanotubes (CNTs) are of great interest because their structure at the nanometer to micrometer scale can be well controlled for supercapacitor applications.<sup>72–74</sup> For instance, a solution layer-by-layer self-assembly approach (Figure 5a–b) was used to prepare multilayered hybrid carbon films of poly(ethyleneimine)-modified graphene sheets and acid-oxidized multiwalled CNTs to construct supercapacitors with an average specific capacitance of 120,000 F/kg.<sup>72</sup>

Similarly, the inherently nanoporous three-dimensional pillared vertically aligned carbon nanotube (VA-CNT)–graphene hybrid architecture with a large surface area (Figure 5c) should allow the selection of specific thermal, mechanical, and electrical properties that are useful for many potential applications, including supercapacitors.<sup>64</sup> To test this possibility, Feng et al.<sup>74</sup> prepared a VA-CNT–graphene hybrid by the intercalated growth of VA-CNTs into thermally expanded highly ordered pyrolytic graphite (Figure 5d). The resulting VA-CNT–graphene hybridized with a nickel hydroxide coating indeed showed a high specific capacitance with an impressive charging-rate capability (Figure 5e).

### Lithium-ion batteries

Lithium-ion batteries are regarded as highly attractive rechargeable batteries because of their low weight and high energy-storage capacity. Typically, a lithium-ion battery is composed of a lithium intercalation anode and cathode and an electrolyte (Figure 6a). The nature and microstructure of the electrode materials are

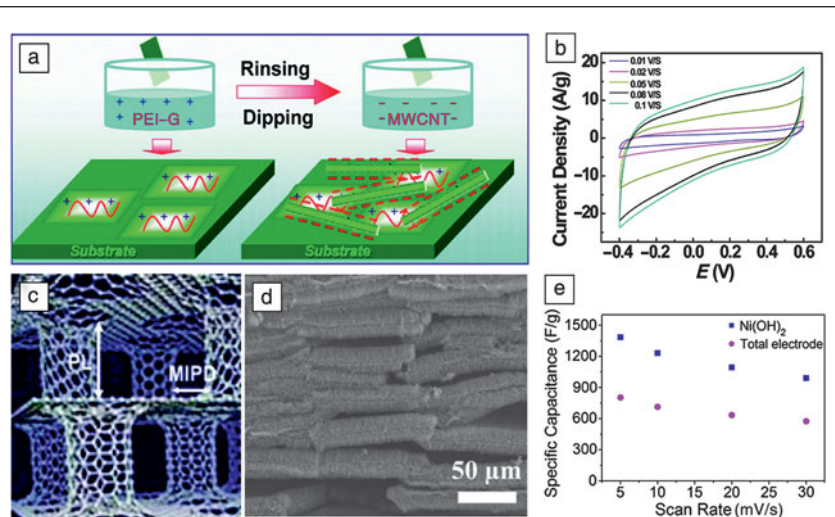


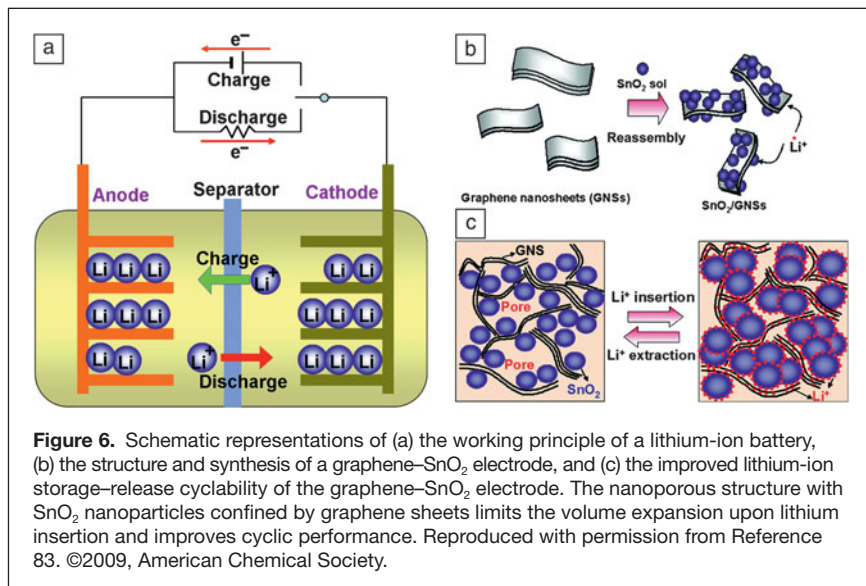
**Figure 5.** (a) Schematic illustration of the preparation of multilayered graphene–multiwalled carbon nanotube (MWCNT) hybrid electrodes for supercapacitors. PEI-G, poly(ethyleneimine)-modified graphene. (b) Cyclic voltammograms from the graphene–MWCNT hybrid electrode in 1.0 M H<sub>2</sub>SO<sub>4</sub> solution. Parts (a) and (b) reproduced with permission from Reference 72. ©2010, American Chemical Society. (c) Schematic illustration and (d) typical scanning electron microscopy image of a three-dimensional pillared vertically aligned carbon nanotube (VA-CNT)–graphene nanostructure. In (c), the dimensions of interest are the pillar length (PL) and the minimum interpillar distance (MIPD). (e) Average specific capacitance of a Ni(OH)<sub>2</sub>-coated VA-CNT–graphene pillared electrode at various scan rates. Parts (c)–(e) reproduced with permission from Reference 74. ©2011, American Chemical Society.

crucial not only for energy and power density but also for battery safety and cycle lifetime.<sup>75,76</sup> Current electrode materials, including carbon black and nanofibers, graphite, silicon, metals, and metal oxides, suffer from poor electrical conductivity and/or huge volume changes during charging/discharging.<sup>75,76</sup>

### Lithium-ion batteries with graphene electrodes

Compared with the widely used graphite electrode, graphene has a larger specific surface area and twice the lithium storage capacity.<sup>77</sup> Moreover, recent work indicated that the graphene two-dimensional edge plane site could aid lithium-ion adsorption and diffusion, leading to a reduced charging time and an increased power output.<sup>78</sup> The nanosized holes in graphene sheets were also found to be responsible for the high-rate discharge capability of lithium-ion battery anodes.<sup>79</sup> Indeed, Pan et al.<sup>78</sup> employed graphene-sheet-based electrodes in lithium-ion batteries and achieved a capacity of 540 A h/kg, which is higher than that of graphite. When carbon nanotubes and fullerenes were used as spacers to prevent individual graphene sheets from restacking, the capacity of the graphene electrodes could be further increased to 730 A h/kg and 784 A h/kg, respectively.<sup>80</sup>

Wu et al.<sup>81</sup> used nitrogen- or boron-doped graphene to realize simultaneous high power and energy densities. The superior performance came from rapid surface Li<sup>+</sup> absorption, ultrafast Li<sup>+</sup> diffusion and electron transport, increased intersheet distance, and improved electrical conductivity because of the two-dimensional structure, disordered surface morphology,



materials with tailor-made microstructures and electrochemical properties for the technological marketplace could lead to a wide range of important uses for graphene materials in high-performance energy-conversion and -storage devices.

## Acknowledgments

The authors are grateful for the financial support from AFOSR (FA9550-12-1-0069, FA9550-09-1-0331, FA9550-10-1-0546, FA8650-07-D-5800, FA2386-10-1-4071, TSI-2356-10-81529, AOARD-104055), DOD-AFOSR-MURI (FA9550-12-1-0037), AFRL/UTC (11-S587-1000-01-C1), AFRL/DAGSI (RX2-CWRU-10-1), US AFOSR-Korea NBIT, US Army (W911NF-11-1-0209), NSF (CMMI-1000768, CMMI-1047655, DMR-1106160), and DOE (DE-SC0003736).

heteroatomic defects, and better electrode/electrolyte wettability of the doped graphene. However, it should be noted that graphene as a lithium-ion battery electrode still suffers from irreversible reactions with lithium and solid electrolyte interface formation, resulting in irreversible performance.<sup>82</sup>

## Lithium-ion batteries with graphene hybrid electrodes

To address the issues discussed in the preceding subsection and to utilize the high lithium-ion reversible storage capacity of metals and metal oxides, graphene electrodes hybridized with certain metal or metal-oxide nanoparticles have been prepared to exhibit improved performance.<sup>83–86</sup> For example, an electrode made of nanoporous graphene sheets decorated with loosely packed SnO<sub>2</sub> nanoparticles (Figure 6b–c) was found to exhibit a reversible capacity of 810 A h/kg with a much improved reversible cycling performance compared to those of bare graphene, SnO<sub>2</sub> nanoparticle, and bare graphite electrodes.<sup>83</sup> Other metal oxides, such as Co<sub>3</sub>O<sub>4</sub>, Fe<sub>2</sub>O<sub>3</sub>, TiO<sub>2</sub>, and SiO<sub>2</sub> have also been used to functionalize graphene for use as electrodes in high-performance lithium-ion batteries.<sup>84–86</sup>

## Concluding remarks

As discussed herein, the intensive study of graphene materials with unique structures and properties offers a great opportunity to meet the challenges of energy conversion and storage. This article presented a critical and concise review of the recent progress in this active emerging area. Even this brief review reveals the versatility of graphene, with and without functionalization, for improving the performance of various energy-conversion (e.g., solar cells, fuel cells) and -storage (e.g., supercapacitors, batteries) devices. Before these materials can be widely adopted, important hurdles must be surmounted, such as processability, scalability, energy capacity, rate capability, and cost effectiveness. However, judicious application of various physicochemical approaches to the development of graphene

## References

1. T.G. Doung, "FY 2002 Annual Progress Report for Energy Storage Research and Development" (FreedomCAR and Vehicle Technologies Program, US Department of Energy, Washington, DC, 2003).
2. L. Dai, *Carbon Nanotechnology: Recent Developments in Chemistry, Physics, Materials Science and Device Applications* (Elsevier Science, London, 2006).
3. K. Novoselov, A. Geim, S. Morozov, D. Jiang, Y. Zhang, S. Dubonos, I. Grigorieva, A. Firsov, *Science* **306**, 666 (2004).
4. A.K. Geim, K.S. Novoselov, *Nat. Mater.* **6**, 183 (2007).
5. K.V. Emtsev, A. Bostwick, K. Horn, J. Jobst, G.L. Kellogg, L. Ley, J.L. McChesney, T. Ohta, S.A. Reshanov, J. Röhrli, E. Rotenberg, A.K. Schmid, D. Waldmann, H.B. Weber, T. Seyller, *Nat. Mater.* **8**, 203 (2009).
6. A. Reina, X. Jia, J. Ho, D. Nezich, H. Son, V. Bulovic, M.S. Dresselhaus, J. Kong, *Nano Lett.* **9**, 30 (2009).
7. G. Eda, M. Chhowalla, *Adv. Mater.* **22**, 2392 (2010).
8. M. Lotya, Y. Hernandez, P.J. King, R.J. Smith, V. Nicolosi, L.S. Karlsson, F.M. Blighe, S. De, Z. Wang, I.T. McGovern, G.S. Duesberg, J.N. Coleman, *J. Am. Chem. Soc.* **131**, 3611 (2009).
9. X. Wang, L. Zhi, N. Tsao, Z. Tomović, J. Li, K. Müllen, *Angew. Chem., Int. Ed.* **47**, 2990 (2008).
10. L. Qu, Y. Liu, J.B. Baek, L. Dai, *ACS Nano* **4**, 1321 (2010).
11. S. Stankovich, D.A. Dikin, G.H.B. Dommett, K.M. Kohlhaas, E.J. Zimney, E.A. Stach, R.D. Piner, S.T. Nguyen, R.S. Ruoff, *Nature* **442**, 282 (2006).
12. Y. Sun, Q. Wu, G. Shi, *Energy Environ. Sci.* **4**, 1113 (2011).
13. X. Huang, Z. Yin, S. Wu, X. Qi, Q. He, Q. Zhang, Q. Yan, F. Boey, H. Zhang, *Small* **7**, 1876 (2011).
14. D.A.C. Brownson, D.K. Kampouris, C.E. Banks, *J. Power Sources* **196**, 4873 (2011).
15. M. Pumera, *Energy Environ. Sci.* **4**, 668 (2011).
16. J. Liu, G. Cao, Z. Yang, D. Wang, D. Dubois, X. Zhou, G.L. Graff, L.R. Pederson, J.G. Zhang, *ChemSusChem* **1**, 676 (2008).
17. C. Liu, F. Li, L.-P. Ma, H.-M. Cheng, *Adv. Mater.* **22**, E28 (2010).
18. A. Becquerel, *C.R. Acad. Sci.* **9**, 561 (1839).
19. R.H. Bube, *Photoelectronic Properties of Semiconductors* (Cambridge University Press, Cambridge, UK, 1992).
20. M.A. Green, K. Emery, D.L. King, S. Igar, W. Warta, *Prog. Photovoltaics Res. Appl.* **12**, 365 (2004).
21. R.M. Swanson, *Prog. Photovoltaics Res. Appl.* **14**, 443 (2006).
22. J. Johnson, *Chem. Eng. News* **82**, 13 (2004).
23. F.C. Krebs, *Polymer Photovoltaics: A Practical Approach* (SPIE Press, Bellingham, WA, 2008).
24. S. Sun, N.S. Sariciftci, *Organic Photovoltaics: Mechanisms, Materials, and Devices* (CRC Press, Boca Raton, FL, 2005).
25. C.W. Tang, *Appl. Phys. Lett.* **48**, 183 (1986).
26. G. Yu, J. Gao, J.C. Hummelen, F. Wudl, A.J. Heeger, *Science* **270**, 1789 (1995).
27. R. Steim, F.R. Kogler, C.J. Brabec, *J. Mater. Chem.* **20**, 2499 (2010).
28. Y. Wang, S.W. Tong, X.F. Xu, B. Özyilmaz, K.P. Loh, *Adv. Mater.* **23**, 1514 (2011).

29. G. Jo, S.I. Na, S.H. Oh, S. Lee, T.S. Kim, G. Wang, M. Choe, W. Park, J. Yoon, D.Y. Kim, Y.H. Kahng, T. Lee, *Appl. Phys. Lett.* **97**, 213301 (2010).

30. S. Bae, H. Kim, Y. Lee, X.F. Xu, J.-S. Park, Y. Zheng, J. Balakrishnan, Y. Lei, H.R. Kim, Y.I. Song, Y.J. Kim, B. Özyilmaz, J.H. Ahn, B.H. Hong, S. Lijima, *Nat. Nanotechnol.* **5**, 574 (2010).

31. S.S. Li, K.H. Tu, C.C. Lin, C.W. Chen, M. Chhowalla, *ACS Nano* **4**, 3169 (2010).

32. J. Liu, Y.H. Xue, Y.X. Gao, D.S. Yu, M. Durstock, L.M. Dai, *Adv. Mater.* **24**, 2228 (2012).

33. S. Yeo, J. Kim, H.-G. Jeong, D.-Y. Kim, Y.-J. Noh, S.-S. Kim, B.-C. Ku, S.-I. Na, *Adv. Mater.* **23**, 4923 (2011).

34. D. Yu, Y. Yang, M. Durstock, J.B. Baek, L. Dai, *ACS Nano* **4**, 5633 (2010).

35. D. Yu, K. Park, M. Durstock, L. Dai, *J. Phys. Chem. Lett.* **2**, 1113 (2011).

36. Z. Liu, Q. Liu, Y. Huang, Y. Ma, S. Yin, X. Zhang, W. Sun, Y. Chen, *Adv. Mater.* **20**, 3924 (2008).

37. Y. Li, Y. Hu, Y. Zhao, G. Shi, L. Deng, Y. Hou, L. Qu, *Adv. Mater.* **6**, 776 (2011).

38. P.V. Kamat, *J. Phys. Chem. C* **112**, 18737 (2008).

39. C.X. Guo, H.B. Yang, Z.M. Sheng, Z.S. Lu, Q.L. Song, C.M. Li, *Angew. Chem., Int. Ed.* **49**, 3014 (2010).

40. B. O'Regan, M. Grätzel, *Nature* **353**, 737 (1991).

41. A. Yella, H.-W. Lee, H.N. Tsao, C. Yi, A.K. Chandiran, M.K. Nazeeruddin, E.W.-G. Diao, C.-Y. Yeh, S.M. Zakeeruddin, M. Grätzel, *Science* **334**, 629 (2011).

42. X. Wang, L. Zhi, K. Mullen, *Nano Lett.* **8**, 323 (2008).

43. T. Lin, F. Huang, J. Liang, Y. Wang, *Energy Environ. Sci.* **4**, 862 (2011).

44. Y. Xu, H. Bai, G. Lu, C. Li, G. Shi, *J. Am. Chem. Soc.* **130**, 5856 (2008).

45. L. Kavan, J.-H. Yum, M.K. Nazeeruddin, M. Grätzel, *ACS Nano* **5**, 9171 (2011).

46. N. Yang, J. Zhai, D. Wang, Y. Chen, L. Jiang, *ACS Nano* **4**, 887 (2010).

47. Y.-B. Tang, C.-S. Lee, J. Xu, Z.T. Liu, Z.-H. Chen, Z. He, Y.-L. Cao, G. Yuan, H. Song, L. Chen, L. Luo, H.-M. Chen, W.-J. Zhang, I. Bello, S.-T. Lee, *ACS Nano* **4**, 3482 (2010).

48. X. Yan, X. Cui, B. Li, L.-S. Li, *Nano Lett.* **10**, 1869 (2010).

49. V. Ramani, *Electrochem. Soc. Interface* **15**, 41 (2006).

50. R. Kou, Y.Y. Shao, D.H. Wang, M.H. Engelhard, J.H. Kwak, J. Wang, V.V. Viswanathan, C.M. Wang, Y.H. Lin, Y. Wang, I.A. Aksay, J. Liu, *Electrochem. Commun.* **11**, 954 (2009).

51. R.I. Jafri, N. Rajalakshmi, S. Ramaprabhu, *J. Mater. Chem.* **20**, 7114 (2010).

52. L.F. Dong, R.R.S. Gari, Z. Li, M.M. Craig, S.F. Hou, *Carbon* **48**, 781 (2010).

53. K. Gong, F. Du, Z. Xia, M. Durstock, L. Dai, *Science* **323**, 760 (2009).

54. Y.Y. Shao, S. Zhang, M.H. Engelhard, G.S. Li, G.C. Shao, Y. Wang, J. Liu, I.A. Aksay, Y.H. Lin, *J. Mater. Chem.* **20**, 7491 (2010).

55. I.-Y. Jeon, D. Yu, S.-Y. Bae, H.-J. Choi, D.W. Chang, L. Dai, J.-B. Baek, *Chem. Mater.* **23**, 3987 (2011).

56. D. Geng, Y. Chen, Y. Chen, Y. Li, R. Li, X. Sun, S. Ye, S. Knights, *Energy Environ. Sci.* **4**, 760 (2011).

57. D. Deng, X. Pan, L. Yu, Y. Cui, Y. Jiang, J. Qi, W.-X. Li, Q. Fu, X. Ma, Q. Xue, G. Sun, X. Bao, *Chem. Mater.* **23**, 1188 (2011).

58. Z.W. Liu, F. Peng, H.J. Wang, H. Yu, W.X. Zheng, J. Yang, *Angew. Chem., Int. Ed.* **50**, 3257 (2011).

59. L. Yang, S.J. Jiang, Y. Yu, L. Zhu, S. Chen, X.Z. Wang, Q. Wu, J. Ma, Y.W. Ma, Z. Hu, *Angew. Chem., Int. Ed.* **50**, 7132 (2011).

60. Z. Yang, Z. Yao, G. Li, G. Fang, H. Nie, Z. Liu, X. Zhou, X. Chen, S. Huang, *ACS Nano* **6**, 205 (2012).

61. S. Wang, L. Zhang, Z. Xia, A. Roy, D.W. Chang, J.-B. Baek, L. Dai, *Angew. Chem., Int. Ed.* **51**, 4209 (2012).

62. S. Wang, D. Yu, L. Dai, D.W. Chang, J.-B. Baek, *ACS Nano* **5**, 6202 (2011).

63. L.L. Zhang, X.S. Zhao, *Chem. Soc. Rev.* **38**, 2520 (2009).

64. B.E. Conway, V. Birss, J. Wojtowicz, *J. Power Sources* **66**, 1 (1997).

65. E. Frackowiak, F. Beguin, *Carbon* **39**, 937 (2001).

66. J.P. Zheng, P.J. Cygan, T.R. Jow, *J. Electrochem. Soc.* **142**, 2699 (1995).

67. A. Rudge, J. Davey, I. Raistrick, S. Gottesfeld, J.P. Ferraris, *J. Power Sources* **47**, 89 (1994).

68. M.D. Stoller, S. Park, Y. Zhu, J. An, R.S. Ruoff, *Nano Lett.* **8**, 3498 (2008).

69. Y. Zhu, S. Murali, M.D. Stoller, A. Velamakanni, R.D. Piner, R.S. Ruoff, *Carbon* **48**, 2118 (2010).

70. Y. Zhu, M.D. Stoller, W. Cai, A. Velamakanni, R.D. Piner, D. Chen, R.S. Ruoff, *ACS Nano* **4**, 1227 (2010).

71. Y. Wang, Z. Shi, Y. Huang, Y. Ma, C. Wang, M. Chen, Y. Chen, *J. Phys. Chem. C* **113**, 13103 (2009).

72. D. Yu, L. Dai, *J. Phys. Chem. Lett.* **1**, 467 (2010).

73. G.K. Dimitrakakis, E. Tylanakis, G.E. Foudakis, *Nano Lett.* **8**, 3166 (2008).

74. F. Du, D. Yu, L. Dai, S. Ganguli, V. Varshney, A.K. Roy, *Chem. Mater.* **23**, 4810 (2011).

75. M. Liang, L. Zhi, *J. Mater. Chem.* **19**, 5871 (2009).

76. G. Zhou, D.-W. Wang, F. Li, L. Zhang, N. Li, Z.-S. Wu, L. Wen, G.Q. Lu, H.-M. Cheng, *Chem. Mater.* **22**, 5306 (2010).

77. G. Wang, B. Wang, X. Wang, J. Park, S. Dou, H. Ahn, K. Kim, *J. Mater. Chem.* **19**, 8378 (2009).

78. D. Pan, S. Wang, B. Zhao, M. Wu, H. Zhang, Y. Wang, Z. Jiao, *Chem. Mater.* **21**, 3136 (2009).

79. T. Takamura, K. Endo, L. Fu, Y. Wu, K.J. Lee, T. Matsumoto, *Electrochim. Acta* **53**, 1055 (2007).

80. E. Yoo, J. Kim, E. Hosono, H. Zhou, T. Kudo, I. Honma, *Nano Lett.* **8**, 2277 (2008).

81. Z.-S. Wu, W. Ren, L. Xu, F. Li, H.-M. Cheng, *ACS Nano* **5**, 5463 (2011).


82. D.S. Su, R. Schlogl, *ChemSusChem* **3**, 136 (2010).

83. S.M. Paek, E.J. Yoo, I. Honma, *Nano Lett.* **9**, 72 (2009).

84. Z.S. Wu, W.C. Ren, L. Wen, L.B. Gao, J.P. Zhao, Z.P. Chen, G.M. Zhou, F. Li, H.M. Cheng, *ACS Nano* **4**, 3187 (2010).

85. D.H. Wang, D.W. Choi, J. Li, Z.G. Yang, Z.M. Nie, R. Kou, D.H. Hu, C.M. Wang, L.V. Saraf, J.G. Zhang, I.A. Aksay, J. Liu, *ACS Nano* **3**, 907 (2009).

86. S.L. Chou, J.Z. Wang, M. Choucair, H.K. Liu, J.A. Stride, S.X. Dou, *Electrochem. Commun.* **12**, 303 (2010). □



**SPECTROSCOPY OF MICROSCOPIC SAMPLES**

CRAIC Technologies UV-visible-NIR microscopes and microspectrophotometers are used for imaging and spectral analysis of sub-micron sized features with absorbance, reflectance, fluorescence, emission and polarized illumination. Capabilities include film thickness measurements, colorimetry and high resolution imaging in the UV, visible and NIR regions. **Rapid & accurate** spectra & images of microscopic samples: The Perfect Vision for Science™.

For more information, call 877.UV.CRAIC or visit our website at [www.microspectra.com](http://www.microspectra.com)

**CRAIC TECHNOLOGIES**

©2011 CRAIC Technologies, Inc. San Dimas, California (USA).

NEXT ISSUE

**MRS Bulletin**

JANUARY 2013

Organic single crystals: Addressing the fundamentals of organic electronics

